Supporting Information

Heteroatom-Engineered Black Phosphorus Nanosheets with Ambient Stability for Selective NO_2/NO Detection

*Yen-Ling Wang, Yi-Ting Wu, Shih-Syuan Huang, I-Jung Wang, Chun-Hua Chen**

Y. L. Wang, Y. T. Wu, S. S. Huang, I. J. Wang, C. H. Chen

Corresponding author: Prof. Chun-Hua Chen

Department of Materials Science and Engineering, National Yang Ming Chiao Tung University, 1001 Ta-Hsueh Rd., Hsin-Chu, 30010 Taiwan.

E-mail: ChunHuaChen@nycu.edu.tw

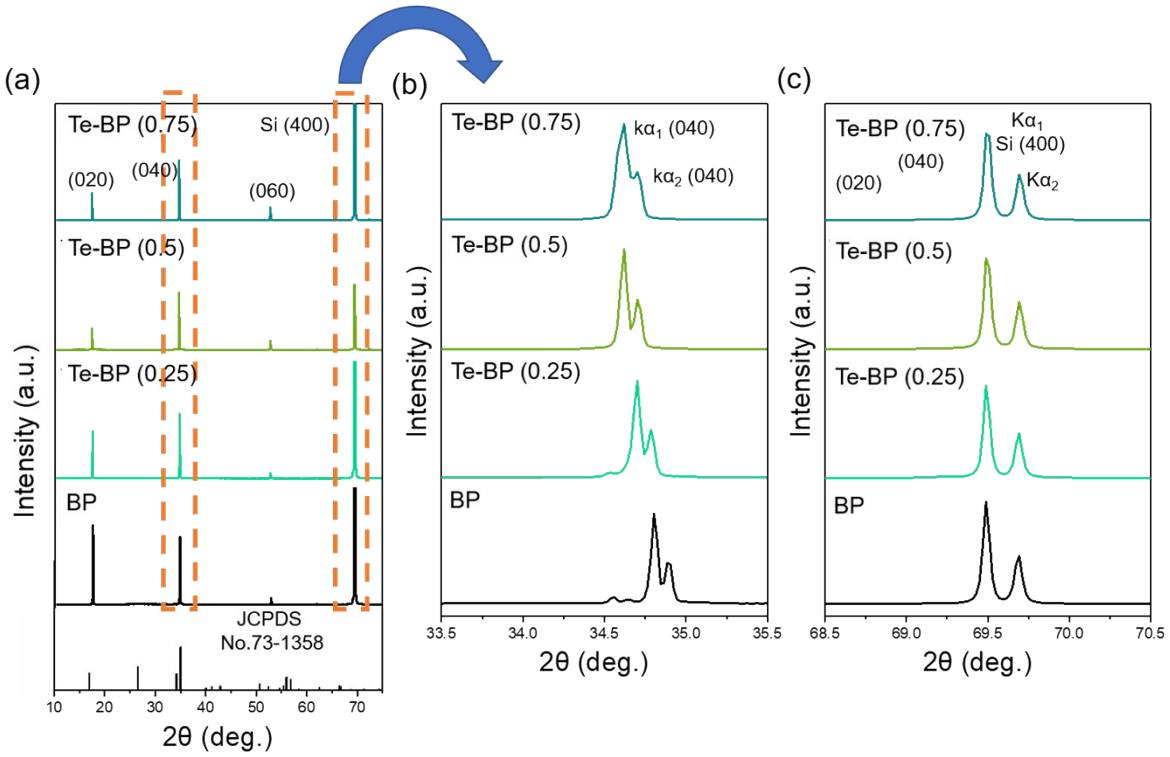

Figure S1. XRD patterns of pristine BP and Te–BP with different Te doping concentrations (0.25, 0.50, and 0.75 at.%). (a) Wide-angle XRD scans; (b,c) enlarged views of the BP(040) reflection and the Si(400) substrate peak, respectively.

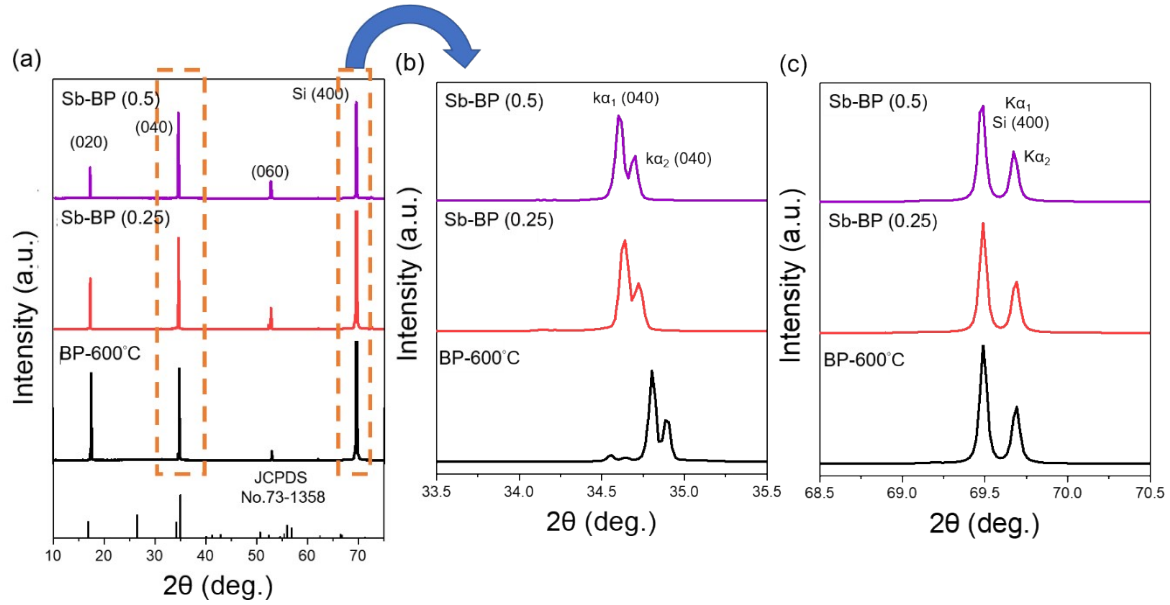

Figure S2. XRD patterns of pristine BP and Te–BP with different Te doping concentrations (0.25, and 0.50 at.%). (a) Wide-angle XRD scans; (b,c) enlarged views of the BP(040) reflection and the Si(400) substrate peak, respectively.

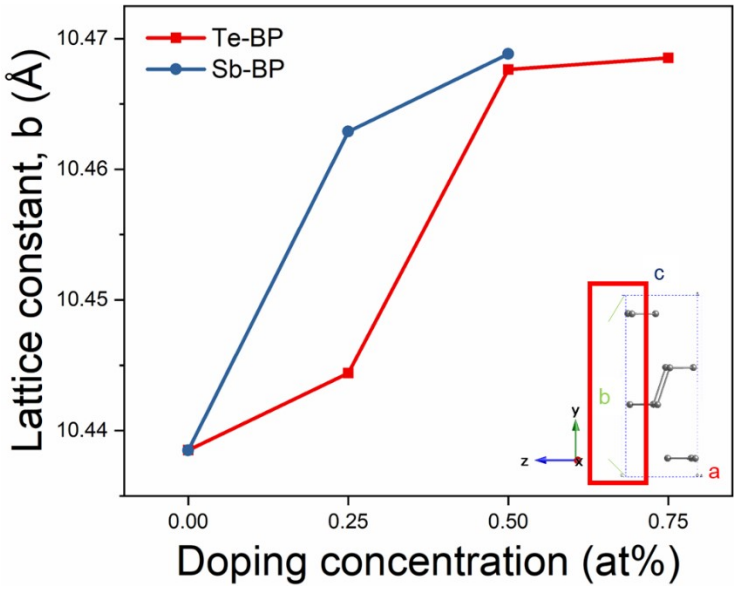

Figure S3. Lattice constant b extracted from the BP(040) XRD peak for Te–BP and Sb–BP with different dopant concentrations (at.%).

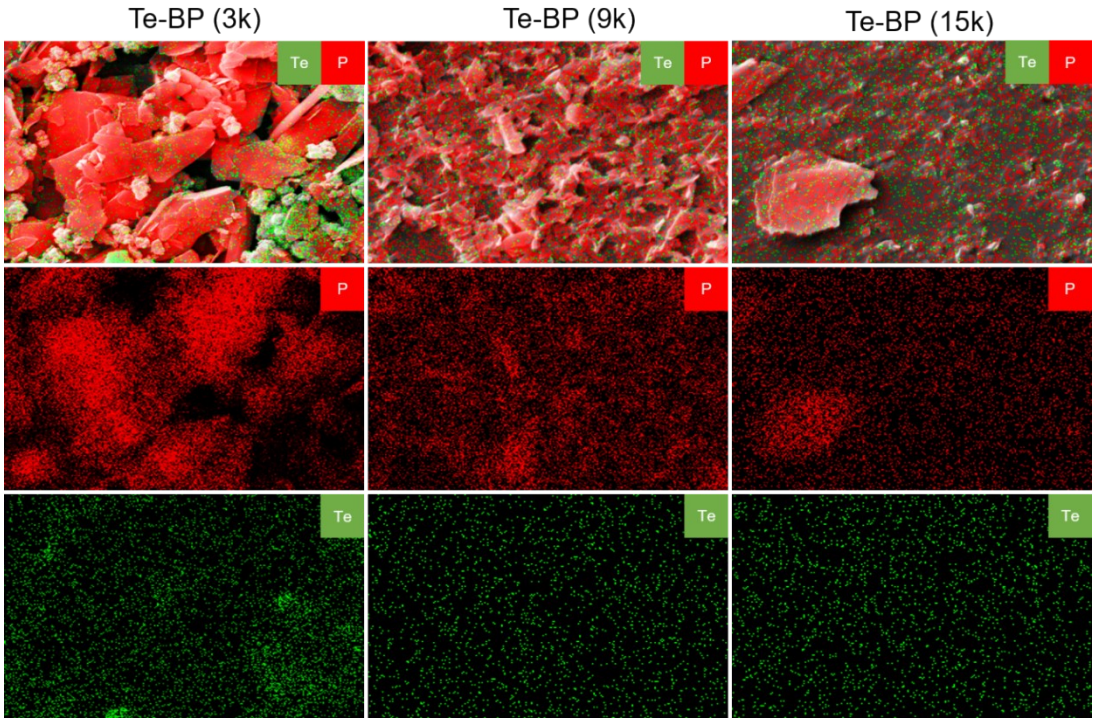

Figure S4. SEM–EDS elemental mapping of Te–BP (3k), Te–BP (9k), and Te–BP (15k), showing the spatial distributions of P and Te.

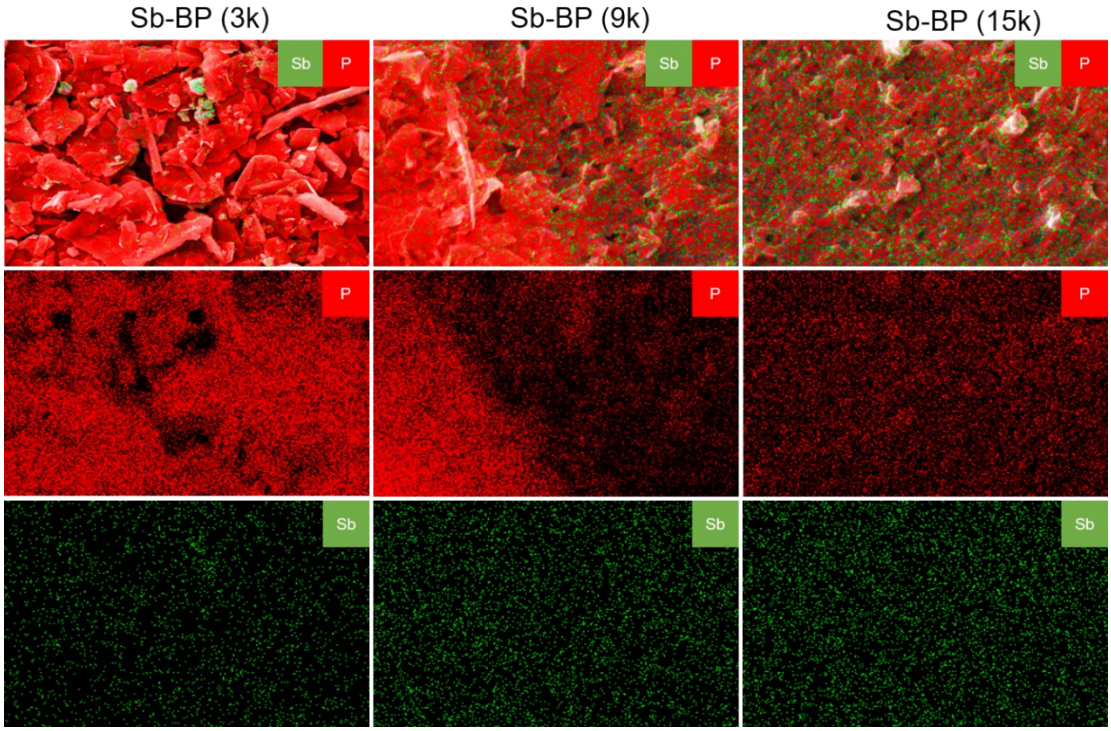

Figure S5. SEM–EDS elemental mapping of Sb–BP (3k), Sb–BP (9k), and Sb–BP (15k), showing the spatial distributions of P and Sb.

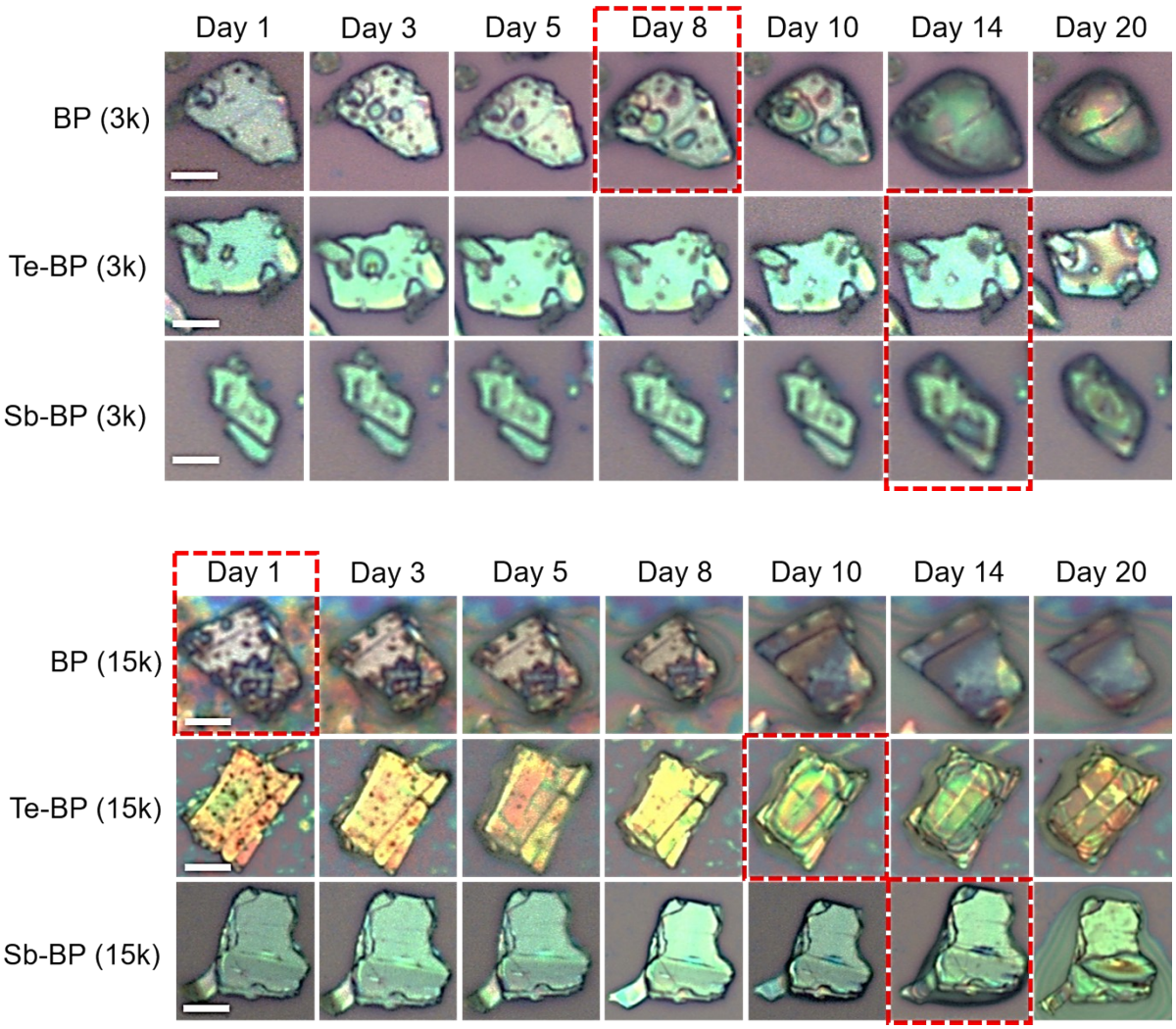

Figure S6. Time-dependent optical microscopy (OM) images of BP, Te–BP, and Sb–BP samples prepared under 3k and 15k conditions during exposure to ambient atmosphere. The morphological and optical contrast evolution was monitored over 20 days. Dashed red boxes highlight representative stages where pronounced degradation or structural changes become evident.

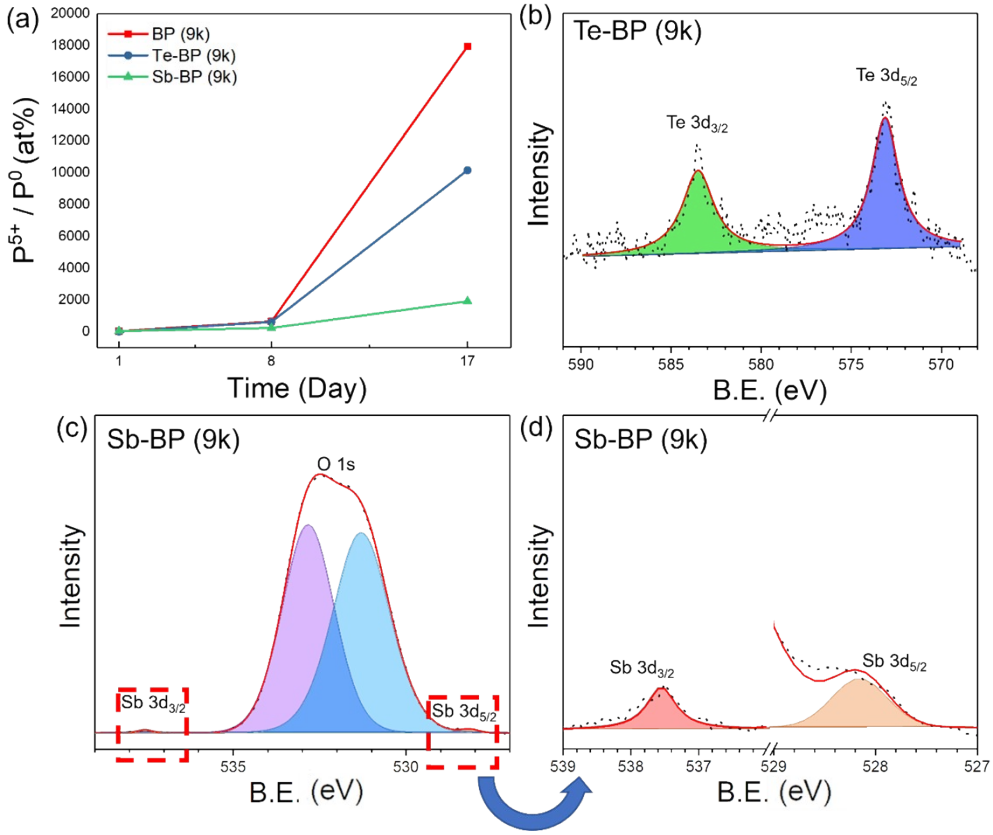

Figure S7. (a) P^{5+}/P^{0} ratios obtained from XPS as a function of air-exposure time for BP (9k), Te–BP (9k), and Sb–BP (9k). (b) Te 3d XPS spectrum of Te–BP (9k). (c) O 1s and Sb 3d overlapping region in Sb–BP (9k). (d) Deconvoluted Sb 3d XPS spectrum of Sb–BP (9k).

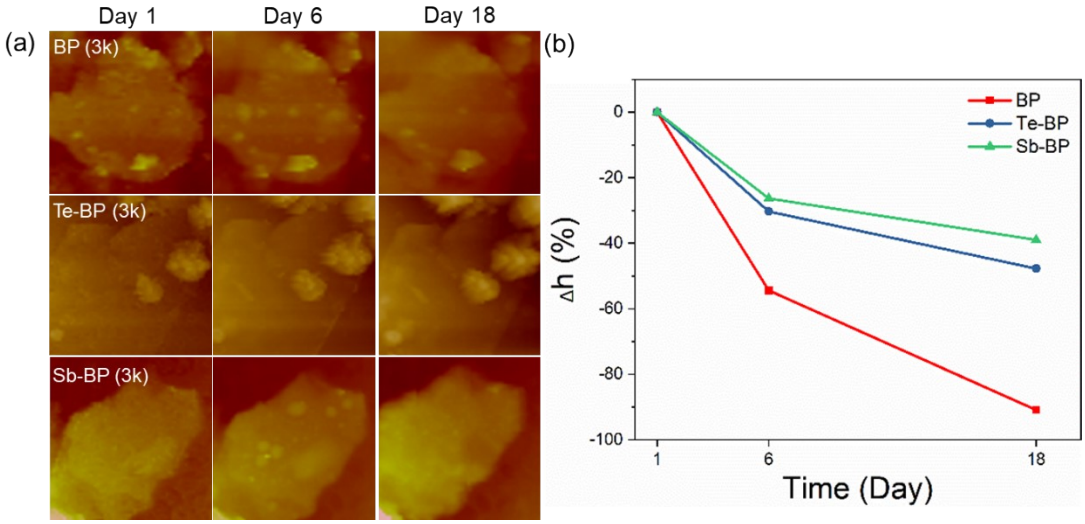

Figure S8. (a) Time-dependent AFM topography images of BP (3k), Te–BP (3k), and Sb–BP (3k) after exposure to ambient air (Day 1, Day 6, and Day 18). (b) Relative thickness change, Δh (%), extracted from the AFM measurements as a function of exposure time for BP, Te–BP, and Sb–BP.

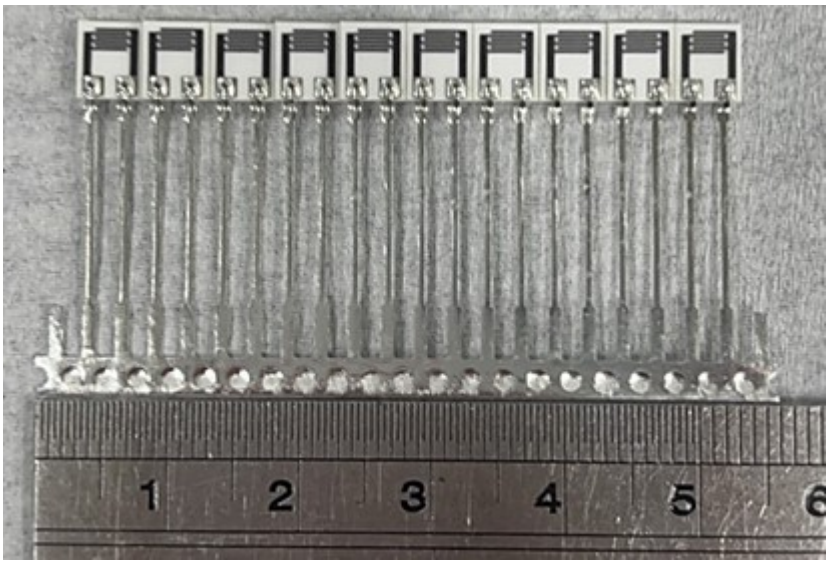

Figure S9. The geometry and dimensions of the substrate for gas sensing measurements.

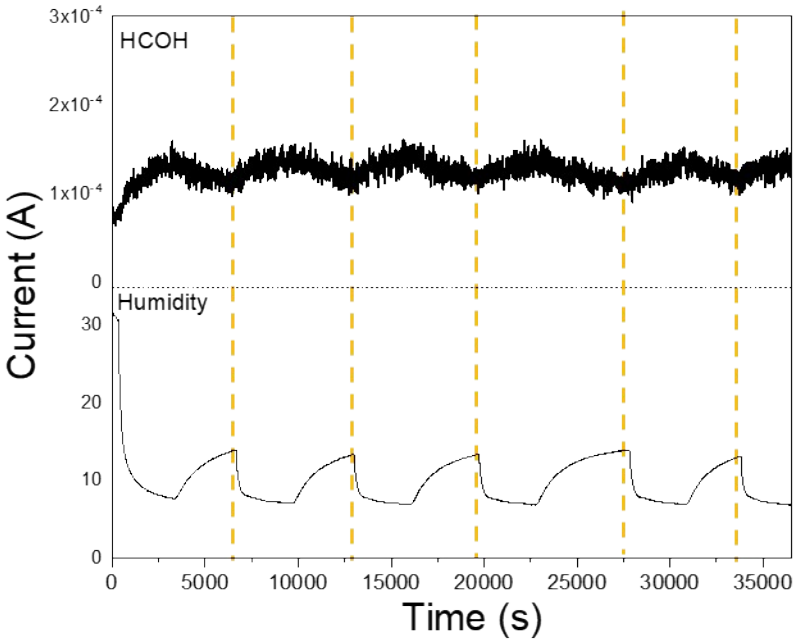

Figure S10. Comparison of the sensing response of BPNSs to HCHO and humidity modulation as a function of time.

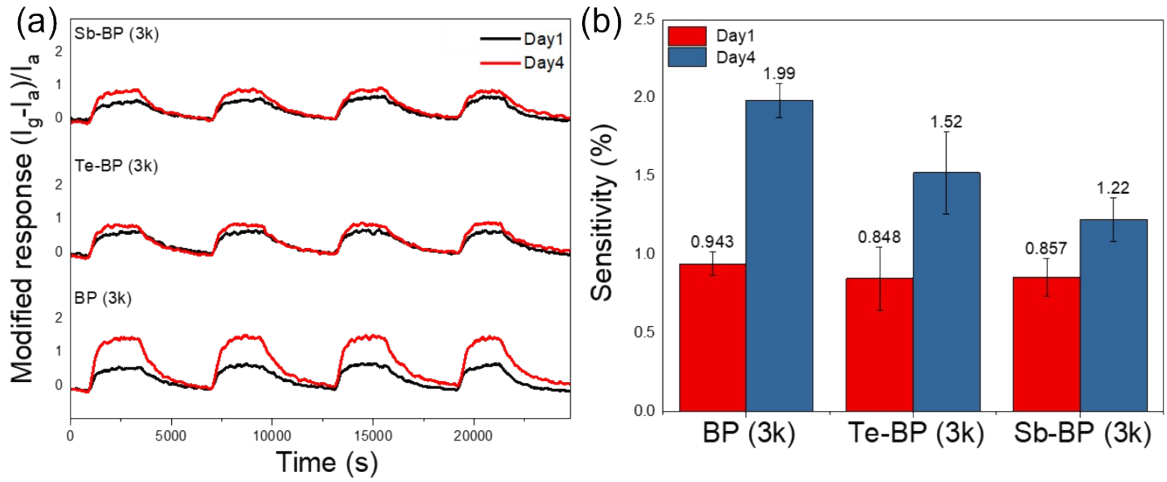

Figure S11. (a) Dynamic sensing responses of BP (3k), Te–BP (3k), and Sb–BP (3k) to 250 ppm NO at room temperature measured on Day 1 and Day 4. (b) Comparison of the sensitivities on Day 1 and Day 4 obtained from repeated measurements

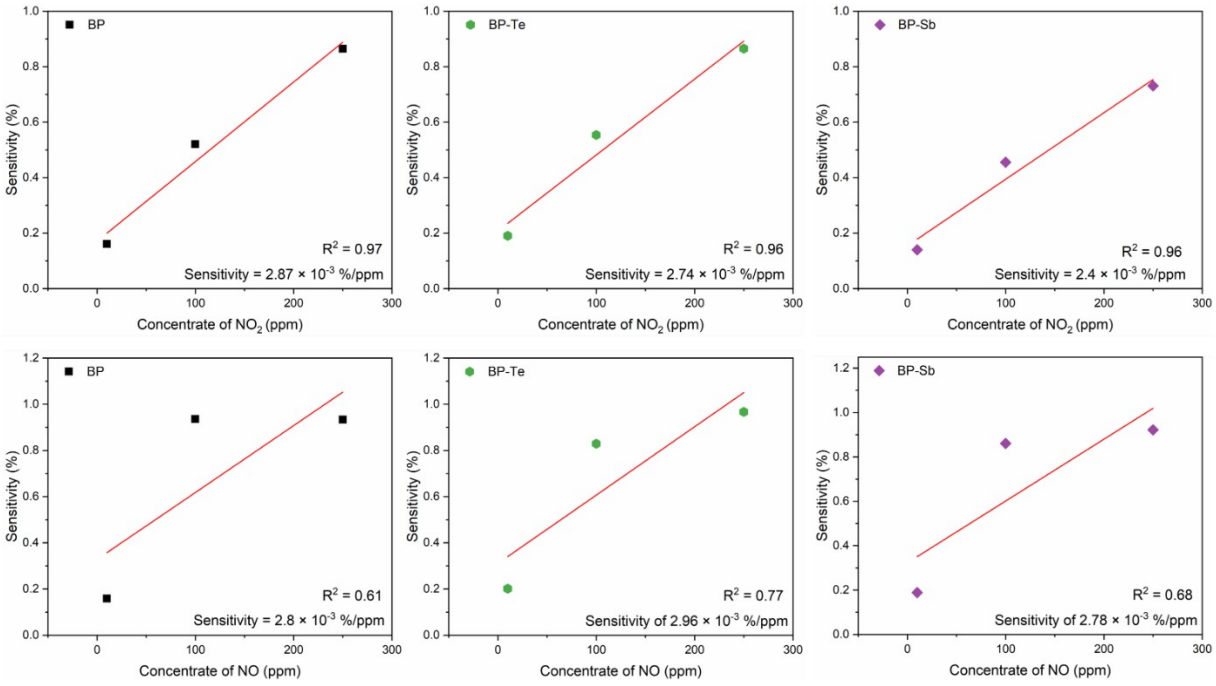

Figure S12. Calibration curves of BP, BP-Te, and BP-Sb for NO and NO_2 gases.

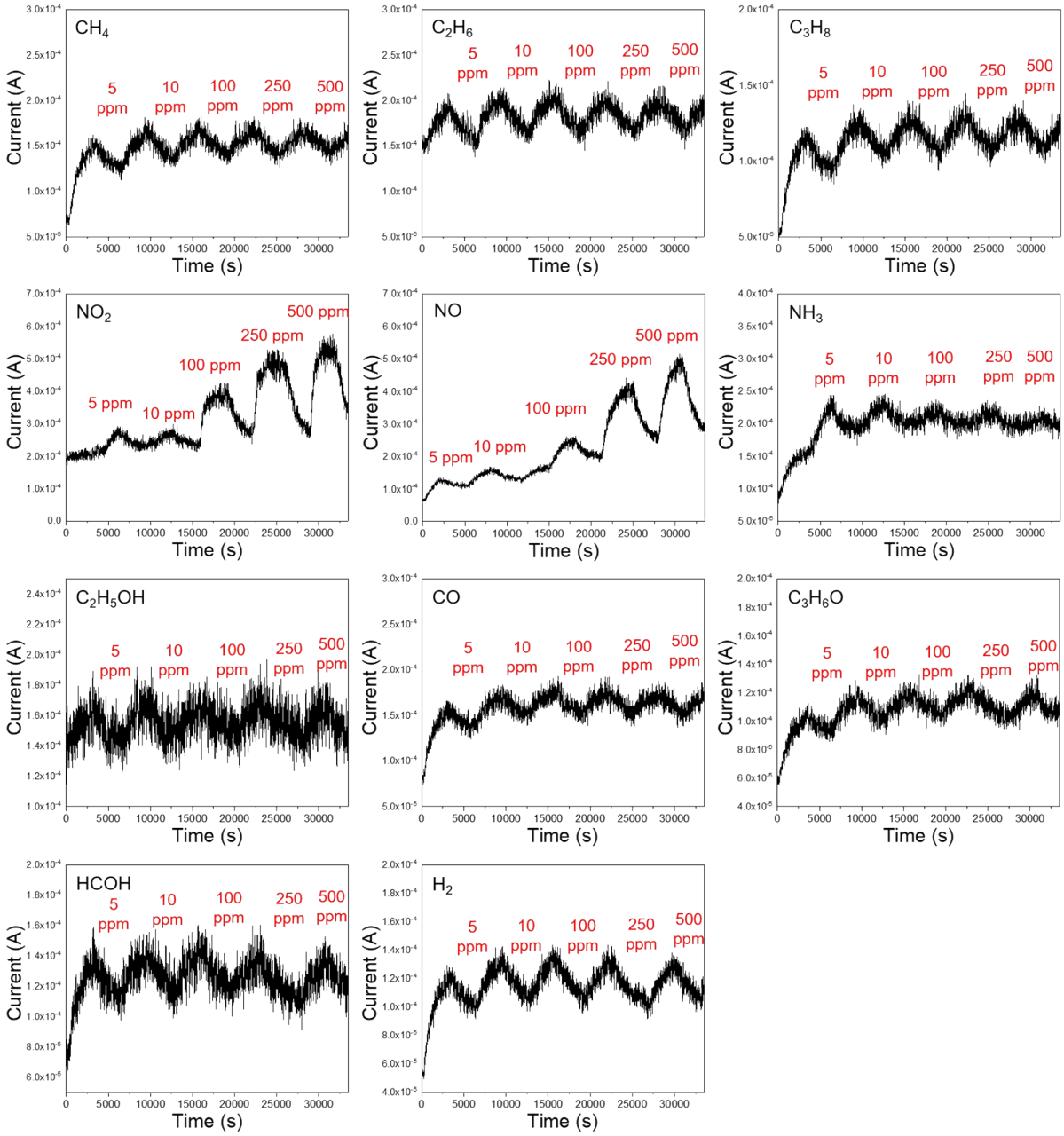

Figure S13. Dynamic sensing responses of BP (3k) to 11 representative gases at various concentrations (5–500 ppm) at room temperature.

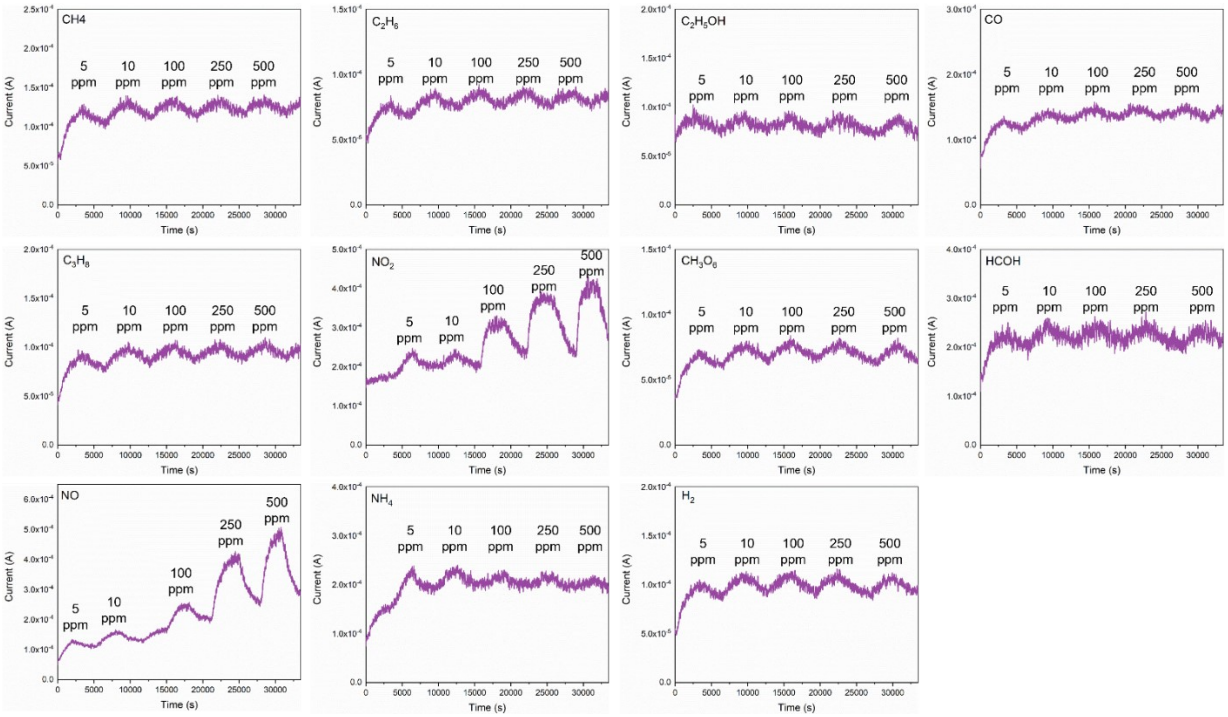

Figure S14. Dynamic sensing responses of BP-Sb (3k) to 11 representative gases at various concentrations (5–500 ppm) at room temperature.

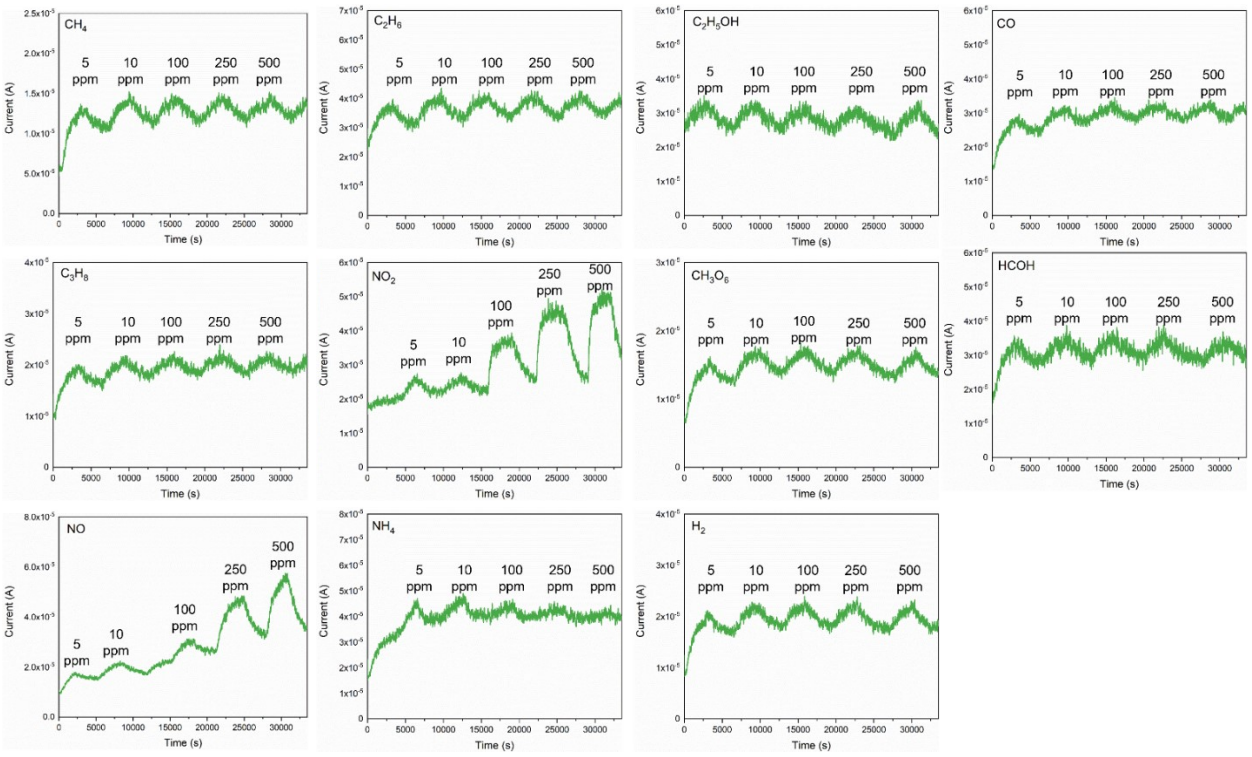

Figure S15. Dynamic sensing responses of BP-Te (3k) to 11 representative gases at various concentrations (5–500 ppm) at room temperature.

Table S1. Lattice parameters and cell volumes of pure BP, Te-doped BP, and Sb-doped BP derived from the XRD analysis.

Sample	a (Å)	b (Å)	c (Å)	V (Å^3)
BP (3k)	3.472	10.375	4.627	166.710
BP-Te (3k)	3.473	10.379	4.640	167.257
BP-Sb (3k)	3.473	10.380	4.637	167.159
BP (9k)	3.472	10.379	4.405	158.783
BP-Te (9k)	3.473	10.378	4.640	167.244
BP-Sb (9k)	3.473	10.383	4.341	156.553
BP (15k)	3.472	10.379	4.637	167.159
BP-Te (15k)	3.474	10.384	4.655	167.935
BP-Sb (15k)	3.472	10.379	4.628	166.845

Table S2. The gas sensing performance of NO for BP, BP-Te, and BP-Sb.

Sample	Response	Response time (s)	Recovery time (s)
BP	0.93	585	2470
BP-Te	0.97	419	1625
BP-Sb	0.92	525	1540

Table S3. The gas sensing performance of NO_2 for BP, BP-Te, and BP-Sb.

Sample	Response	Response time (s)	Recovery time (s)
BP	0.86	685	2277
BP-Te	0.87	482	1619
BP-Sb	0.73	351	1915